Journal of Quantitative Spectroscopy & Radiative Transfer 191 (2017) 40–45

Contents lists available at ScienceDirect

Journal of Quantitative Spectroscopy & Radiative Transfer

journal homepage: www.elsevier.com/locate/jqsrt

Ultraviolet scattering properties of alumina particle clusters at three phase states in aircraft plume

Jingying Li [a], Lu Bai [a,b,*], Zhensen Wu [a,b], Lixin Guo [a,b], Yanjun Gong [c]

[a] School of Physics and Optoelectronic Engineering, Xidian University, Xi'an 710071, Shaanxi, China
[b] Collaborative Innovation Center of Information Sensing and Understanding at Xidian University, China
[c] School of Electronics and Information Engineering, Hunan University of Science and Engineering, Yongzhou, 425199 Hunan, China

ARTICLE INFO

Article history:
Received 23 September 2016
Received in revised form
13 January 2017
Accepted 13 January 2017
Available online 19 January 2017

Keywords:
Clustered alumina particle
Scattering property
Phase state
Ultraviolet

ABSTRACT

We simulate the clusters of alumina particles using the parallel diffusion limited aggregation algorithm (DLA), and solve the scattering matrixes of the alumina particles in different phase states (alpha phase, gamma phase and liquid) through the multiple sphere T matrix method in UV. The effect of the number of monomers, fractal dimension and incident wavelength to the scattering phase function of the clusters of alumina particles is discussed. The results show that the different of the number of monomers, fractal dimensions and incident wavelengths have significant effect on the scattering properties of the clustered alumina particle. The researchers used to make the alumina particle equivalent to the alpha phase spherical particle, but it is too simplistic. We compare the scattering phase functions of the equivalent volume sphere (EVS), the equivalent surface sphere (ESS) and the clusters of alumina particles in three kinds of phase states. The results show that the backward scattering would be overestimated if the alumina particle is equivalent to the alpha phase spherical particle. Accurate phase function calculation in different phase states is very helpful to study the radiation propagation characteristics of aircraft plume.

1. Introduction

Recently, the scattering and radiation propagation characteristic of aircraft plume have attracted attention widely. Rankin [1] assessed the results of narrowband radiation and combustion models according the radiation intensity. Pan [2] applied the radiation characteristic for predicting the invisible aircraft. Meanwhile, alumina particle is an important component of the plume. In the plume, the alumina particle will become clustered [3]. Song [4] measured the absorption coefficient and the size distribution of clustered alumina particle by experiment. Plastinin [5] thought that the alumina particles will experience lots of phase states, such as alpha, gamma, θ, δ, κ and liquid, but liquid, gamma phase and alpha phase only are the most stable phase state in the plume. Dill [6] pointed out alpha and gamma phase alumina particles exist in the plume of rocket motor and gave the percentage of each phase state.

Rodionov's research [7] showed the radiation propagation characteristic will be obtained if there are optical parameters of the alumina particles in the different phase states. Konopka et al. [8] measured and determined the particle size of alumina particle in plume of solid rocket motor by laser and scanning electronic microscope. Yang [9] predicted the high temperature optical absorption of alpha phase alumina according the AIMD method. Plastinin [10,11] thoroughly studied the effect of the different phase states to the UV and MIR radiation characteristic. Zhang [12] considered Al_2O_3 particle is the major radiation composition in the plume, whose scattering coefficient is much larger than its absorption coefficient. However, the alumina particle was simplified to alpha phase spherical particle in above research. Parry [13] shown the gamma phase and the liquid have higher absorption index, and considered these alumina particles accounted for a larger proportion in the plume. Therefore, it is obviously not enough to only study the scattering property of the alpha phase alumina particle.

In this paper, we simulate clustered alumina particles instead of sphere and discuss the characteristic of clustered alumina in different phase states. In Section 2, detailed explanation of the DLA algorithm is described. In Section 3, the theory of multiple sphere T matrix method is introduced, and the results of numerical calculations will be shown in Section 4. Finally, Section 5 is summary and conclusion of the paper.

2. Clustered alumina particles simulation

The alumina particles are simulated using DLA algorithm [14,15]. The construction and morphology of the fractal clusters

* Corresponding author.
E-mail address: blu@xidian.edu.cn (L. Bai).

http://dx.doi.org/10.1016/j.jqsrt.2017.01.018
0022-4073/

can be described by the statistical scaling law [16,17]:

$$Ns = k_f \left(\frac{R_g}{a} \right)^{D_f} \quad (1)$$

$$R_g^2 = \frac{1}{Ns} \sum_{i=1}^{Ns} r_i^2 \quad (2)$$

where Ns is the number of the monomers in the cluster, a is the mean radius of the monomer, k_f is the fractal prefactor D_f is the fractal dimension, R_g is the radius of gyration, which represents the deviation of the overall aggregate radius in a cluster, $r_i$is the distance from the ith monomer to the center of the cluster.

The fractal prefactor, k_f, and the fractal dimension, D_f, are the two most important parameters in the determination of the geometries of aggregates. In this study, the value of the parameter is assumed to be $k_f = 1.2$, chosen from results reported in the literature [18]. The mean radius of the alumina monomers is 100 nm [7]. Fig. 1 shows the typical scanning electron microscope photo of alumina particles in the plume and some examples of the alumina fractal aggregates are simulated using the DLA algorithm.

3. Multiple sphere T matrix method

The multiple sphere T matrix method has become an important numerical tool for computing the random-orientation scattering matrix of the clustered particles. The procedure for analytically calculating the T matrix for a cluster of spheres has been described in detail in Mackowski [19], only an outline of the formulation will be presented here. The scattered field from the cluster as a whole is resolved into partial fields scattered from each of the Ns sphere in the cluster, i.e.,

$$\mathbf{E}^{sca}(\boldsymbol{r}) = \sum_{j=1}^{Ns} \boldsymbol{E}_j^{sca}(\boldsymbol{r}) \quad (3)$$

where $\boldsymbol{E}_j^{sca}$ is the scattered flied for sphere j and $\boldsymbol{r}$ connects the origin of the common coordinate system and the observation point.

The field arriving at the surface of the jth sphere will consist of the incident field plus scattered fields that originate from all other spheres in the cluster. For the jth sphere, the incident filed $\boldsymbol{E}_j^{inc}$ is expressed as follows:

$$\boldsymbol{E}_j^{inc}(\boldsymbol{r}) = \boldsymbol{E}_0^{inc}(\boldsymbol{r}) + \sum_{l=1,l\neq j}^{Ns} \boldsymbol{E}_l^{sca}(\boldsymbol{r}) \; j=1, \ldots, Ns \quad (4)$$

In the above equation $\boldsymbol{E}_0^{inc}(\boldsymbol{r})$denotes the external incident filed. To get the T matrix of the jth sphere, the incident field and the scattered filed are expanded in vector spherical wave functions as following:

$$\boldsymbol{E}_j^{inc}(\boldsymbol{r}) = \sum_{n,m} \left[\left(a_{nm}^{j0} + \sum_{l=1,l\neq j}^{Ns} a_{nm}^{jl} \right) R_g \boldsymbol{M}_{mn}(k_1 \boldsymbol{r}_j) + \left(b_{nm}^{j0} + \sum_{l=1,l\neq j}^{Ns} b_{nm}^{jl} \right) R_g \boldsymbol{N}_{mn}(k_1 \boldsymbol{r}_j) \right] \quad (5)$$

$$\boldsymbol{E}_j^{sca}(\boldsymbol{r}) = \sum_{n,m} [p_{nm}^j \boldsymbol{M}_{mn}(k_1 \boldsymbol{r}_j) + q_{nm}^j \boldsymbol{N}_{mn}(k_1 \boldsymbol{r}_j)] \; j=1, \ldots Ns \quad (6)$$

where $\boldsymbol{r}_j$ connects the origin of the jth local coordinate system and the observation point. Owing to the linearity of Maxwell's equations and boundary conditions, the relationship between the scattered field expanding coefficients and the incident field expanding coefficients is given by $\boldsymbol{T}^j$matrix:

$$\begin{bmatrix} \boldsymbol{p}^j \\ \boldsymbol{q}^j \end{bmatrix} = \boldsymbol{T}^j \left(\begin{bmatrix} \boldsymbol{a}^{l0} \\ \boldsymbol{b}^{l0} \end{bmatrix} + \sum_{l\neq j} \begin{bmatrix} \boldsymbol{A}(k_1 \boldsymbol{r}_{lj}) & \boldsymbol{B}(k_1 \boldsymbol{r}_{lj}) \\ \boldsymbol{B}(k_1 \boldsymbol{r}_{lj}) & \boldsymbol{A}(k_1 \boldsymbol{r}_{lj}) \end{bmatrix} \begin{bmatrix} \boldsymbol{p}^l \\ \boldsymbol{q}^l \end{bmatrix} \right) \; j = 1, \ldots, N_s \quad (7)$$

where $\boldsymbol{r}_{lj} = \boldsymbol{r}_l - \boldsymbol{r}_j$ connects the origins of the lth and jth local coordinate systems. Inversion of the above equation gives:

$$\begin{bmatrix} \boldsymbol{p}^j \\ \boldsymbol{q}^j \end{bmatrix} = \sum_{l=1}^{Ns} \boldsymbol{T}^{jl} \begin{bmatrix} \boldsymbol{a}^{l0} \\ \boldsymbol{b}^{l0} \end{bmatrix} \; j = 1, \ldots, Ns \quad (8)$$

where the matrix $\boldsymbol{T}^{jl}$ transforms the coefficients of the incident filed expansion centered at the lth origin into the jth-origin-centered expansion coefficients of the partial field scattered by the jth component. Finally, the cluster T matrix is given by

$$\mathbf{T} = \sum_{j,l=1}^{Ns} \begin{bmatrix} R_g\boldsymbol{A}(k_1 \boldsymbol{r}_{j0}) & R_g\boldsymbol{B}(k_1 \boldsymbol{r}_{j0}) \\ R_g\boldsymbol{B}(k_1 \boldsymbol{r}_{j0}) & R_g\boldsymbol{A}(k_1 \boldsymbol{r}_{j0}) \end{bmatrix} \boldsymbol{T}^{jl} \begin{bmatrix} R_g\boldsymbol{A}(k_1 \boldsymbol{r}_{0l}) & R_g\boldsymbol{B}(k_1 \boldsymbol{r}_{0l}) \\ R_g\boldsymbol{B}(k_1 \boldsymbol{r}_{0l}) & R_g\boldsymbol{A}(k_1 \boldsymbol{r}_{0l}) \end{bmatrix} \quad (9)$$

Where k_1 is the wave number of the medium. Then, we can obtain the random orientation scattering matrix elements.

In the standard {I, Q, U, V} representation of polarization, the normalized Stokes scattering matrix has the well known block-diagonal structure [20,21]:

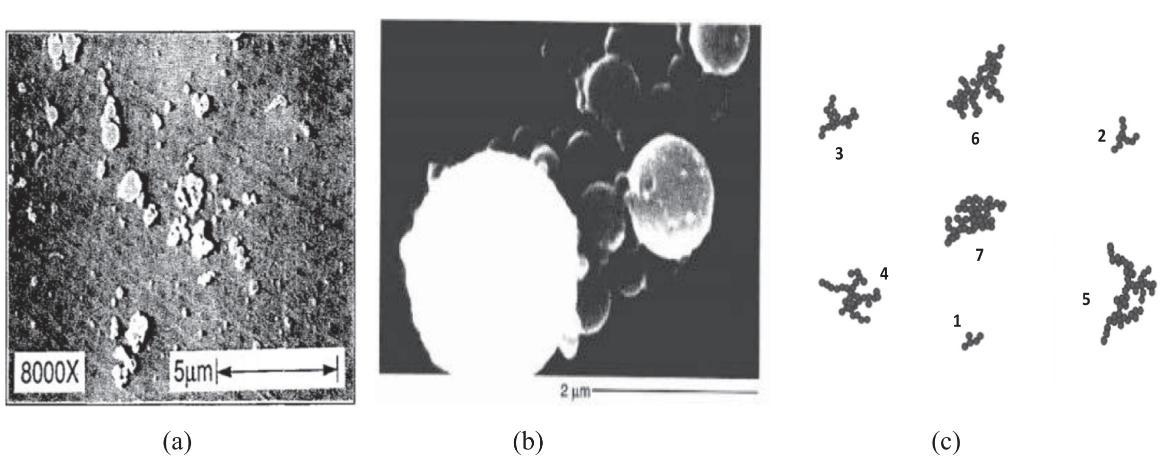

Fig. 1. The pictures of alumina particles in the plume. (a) The typical scanning electron microscope photo of alumina particles in the plume [6]; (b) Alumina particles produced in a rocket motor [3]; (c) Some examples of the alumina fractal aggregates are simulated using the DLA algorithm, The parameters of these particles are: $k_f = 1.2$ and $a = 100$ nm. (1)-(4) $Ns =$ 5, 10, 20 and 35,$D_f =$ 1.82; (5)-(7) $Ns =$ 50, $D_f =$ 1.62, 1.82 and 2.11.